

LRP 789/04

July 2004

**Fracture toughness and tensile
properties of the titanium alloys
Ti6Al4V and Ti5Al2.5Sn before and
after proton and neutron irradiations
at 150°C**

F. Hegedues, R. Brüttsch, B. Oliver, P. Marmy

"Appendice"

*Proton integrated current and DPA determination
for Titanium samples irradiated at PIREX*
F. Hegedues

EFDA TASK TW1-TVV/Titan and TW3-TVM-TICRFA:
Titanium Alloys Irradiation Testing

**Fracture toughness and tensile
properties of the titanium alloys
Ti6Al4V and Ti5Al2.5Sn before and after
proton and neutron irradiations at 150°C**

Centre de Recherche en Physique des Plasmas,
Technologie de la fusion
Association Euratom- Confédération Suisse
Ecole Polytechnique fédérale de Lausanne
5232 Villigen , PSI, Switzerland

prepared by Pierre Marmy

Contributors:

Ferenc Hegedues ++
Roland Brütsch ♣
Brian Oliver ♦
Pierre Marmy

++ X-ray consulting, CH-5232 Villigen

♣ Paul Scherrer Institut, CH-5232 Villigen

♦ Battelle , PNLL, Richland, WA 99352

MAI 2004

Summary:

1. Introduction
2. Origin, structure and chemical analysis of the alloys
3. Microstructure of the as received alloys
4. Experimental
5. Specimen dosimetry
6. Hydrogen measurements in the proton irradiated specimens
- 7.0 Mechanical tests results
- 7.1 Tensile tests results
- 7.2 Fracture Toughness tests results
8. Conclusions

1. Introduction.

The ITER first wall modules are attached to the vacuum vessel by a set of four radial flexibles cartridges. Due to their excellent elasticity and strength properties, titanium alloys have been proposed as materials for fabricating the supports. Among a set of proposed alloys, the European home team is checking the properties of two candidate alloys, the alpha+beta Ti6Al4V and the alpha phase Ti5Al2.5Sn alloy. In the previous CRPP tasks BL14.2 and TWO-T429, the tensile, fatigue and fracture toughness properties have been studied before and after irradiation and also the influence of hydrogen loading up to 400 wppm has been reported (see references[1-4]). The fatigue specimens were irradiated at 350°C with protons and were subsequently tested at 350°C. The fatigue performance was very similar in both alloys. The tensile specimens were irradiated with protons at 40 and 350°C. The Ti6Al4V alloy was found to suffer from serious phase instability when irradiated at 350°C. The fracture toughness properties were similar in both alloys after an irradiation with neutrons at 50 and 350°C. The fracture toughness was strongly reduced at room temperature, in both alloys.

The aim of the task TW1/TVM-Titan is to investigate the effect of two different irradiations with protons and neutrons, on the tensile and fracture toughness properties at 150°C, in the center of the ITER temperature window of the components concerned. The irradiation with protons will generate hydrogen in large quantities in the Ti alloys, with possible detrimental effects on the properties. The subsequent project TW3/TVM/TICRFA was dedicated to the study of the effect on mechanical properties at the same temperature but after neutron irradiation. Because the neutrons do not generate any hydrogen, some specimens were previously loaded with 150 wppm hydrogen. The gained information should allow for an assessment of the combined effect of displacement damage and hydrogen. To assess the effect of alloying on hardening, one tensile specimen of titanium grade 2 (pure titanium) has been added to the proton irradiation matrix.

2. Origin, structure and chemical analysis of the alloys.

The Ti5Al2.4Sn alloy was provided by the SIBER HEGNER & CO. AG, Zürich. The origin of the material is the HOWMET Mill, USA. The material obeys the AMS 4926H specification. After hot forming, it has been annealed 1hr at 815°C and then air cooled. The finished stock is round bar of 31.75 mm. The structure consists of equiaxed grains of 20 µm. The chemical specification is given below.

The Ti6Al4V alloy was bought at Firth-Stahl AG, Dübendorf and comes from the TIMET, Savoie SA in UGINE, France. It was produced according to the specification WL 3.7164.1 and DIN 65040/65174 to a stock diameter of 150mm. After hot forming in the alpha + beta field, it has been annealed for 1.5 hr at 730 °C and then air cooled. The structure consists of equiaxed alpha grains of about 20 µm, containing secondary alpha zones surrounded by beta phase.

The comparison Ti Grade2 material (industrial pure titanium) was supplied by the Siber Hegner & Co in Zürich and comes from Daido Steel, Japan. It corresponds to the standard ASTM B348-GR2 and was delivered as 40mm round bars.

The specimens were cut in the longitudinal direction of the rods, in the L-R or L-C orientation.

Table 1: Chemical compositions: [wt %]

	Al	C	Fe	Sn
Ti Grade 2		0.01	0.07	
Ti5Al2.4Sn	5.0	0.17	0.36	2.4
Ti6Al4V	6.08	0.0056	0.1399	-
H ₂	N ₂	O ₂	V	Others
0.0020	0.010	0.150		<0.4
0.0036	0.010	0.179	-	
<0.0060	0.0065	0.176	3.95	<0.4

3. Microstructure of the as received alloys.

Ti5Al2.5Sn

The Ti5Al2.5Sn alloy has a globular appearance with grains mostly of the order of 20 μm . Some larger grains of about 40 μm or more also exist. Usually the larger grains contain smaller ones. A precipitation of an iron rich phase has been detected in the grains, both by optical and transmission microscopy. The TiFe precipitates have a size around 100 nm and are located at the grain boundaries and inside the grains. They are generated by the high iron concentration in the alloy (0.36 wt%). No hydrides are present in the *as received* microstructure [3, 5].

Ti6Al4V

The Ti6Al4V alloy has a globular structure, composed by primary α grains around 20 μm in size and colonies of secondary elongated α grains, surrounded by intergranular β phase. The fraction volume of the β phase is around 13 %. Due to its different composition the β phase is quite visible at the boundaries and appears as intergranular bands of 0.05 to 1 μm width. Some small quantities of residual martensite can be observed in the larger β grains. No hydrides are observed. [3, 5]

Ti Grade 2

Ti Grade 2 is a single hcp phase material with excellent corrosion resistance. The main strengthening mechanism is from interstitial and impurity atoms. Fe and O are the principal agents controlling the strength. A precise description of the microstructure is currently not available.

4. Experimental details

- *Specimens*

The specimens selected for the fracture toughness is a mini-charpy DIN 50115 KLST with a size of 3x4x27 mm (see Figure 1). The pre/crack of 1mm length was grown before the irradiation (with notch depth 2mm), at high frequency, in a fatigue pre-test. The specimens for the neutron irradiation were cracked after the irradiation, before the test, at low frequency.

The tensile specimens for the proton irradiation were standard PIREX flat specimens with a gauge size of 4x0.34x5.5 mm.

The tensile specimens for the neutron irradiation were DIN 50125 cylindrical specimens with a geometrical gauge length of 18mm and 3 mm diameter.

All specimens were cut in the longitudinal direction of the rods, in the L-R or L-C orientation.

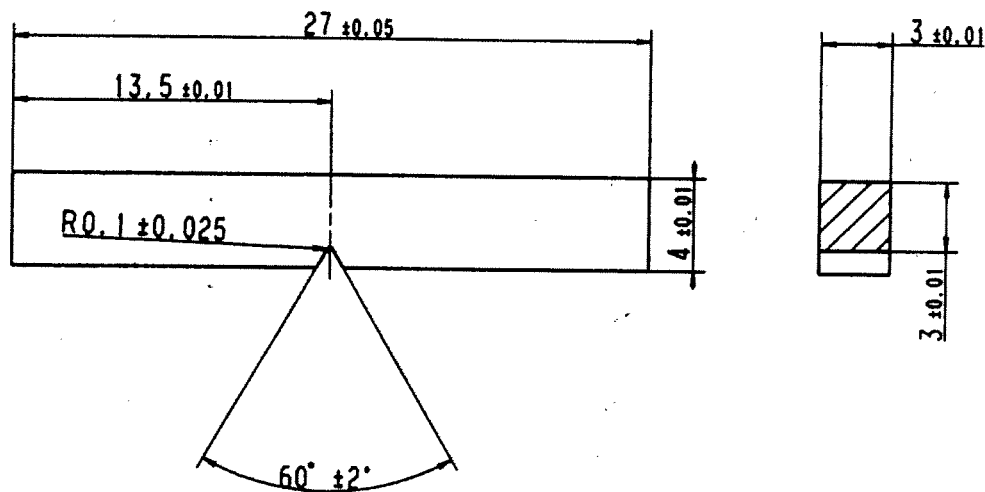


Figure 1. Mini-charpy DIN 50115 KLST

- *Proton Irradiation*

The PIREX facility has been designed to irradiate thin wall materials. The heat deposited by the proton beam is removed by pressurized helium.

Due to the massive dimensions of the charpy specimen, special care was given to beam heating. A new specimen holder was designed to irradiate the 3x4 mm cross section specimen. The mini Charpy specimen was equipped with a central thermoelement placed into an hole that ended very close, at 1.5 mm from the pre/crack. During the irradiation, the temperature was monitored accurately by the thermocouple. A beam with a width of 6mm and a height of 3mm was centered onto the specimen. It was not wobbled because only the center of the specimen had to be irradiated. In the cooling flow of pressurized helium, 115Nm³/hr and 30 bars and 40°C, a beam intensity of 7µa was adjusted to reach an irradiation temperature of 150°C.

The tensile flat specimen was irradiated using a normal specimen holder and the temperature was monitored with a thermocouple welded onto the gauge length. The beam size was 3mm horizontal and 4mm vertical. The wobbler amplitude was ±2.5mm.

The respective irradiation time of each specimen type was chosen such as to reach a dose of approximately 0.10 dpa.

As indicated in the table 2, the PIREX irradiations were conducted in four batches, starting with I25C54, I25C56 and I25C55 on September 28 and finishing November 1, 2001. The second irradiation with the mini charpys I14C54, I14C53 and I14C56 was conducted between October 5 and November 3, 2001. The third irradiation with tensile specimens I31T6, I14T28, I25T12 was conducted from November 9 to Nov 11 2001. The last irradiation was run from Mai 17 to Mai 19 2002, irradiating I25T14, I14T27 and a set of five material dosimeters.

- *Neutron Irradiation*

The neutron irradiation was performed at the Atomic Energy Research Institute in Budapest, between June and November 2002 . The reactor used is a VVRSZM Russian Research Reactor of 10MW power. The mean flux at nominal power is 3.5×10^{13} n/cm² s ($E > 1\text{MeV}$). The neutron spectrum of the reactor is closed to a fission spectrum. The specimens were irradiated using the rig BAGIRA, in which a flow of a He/N₂ gas mixture is used for temperature control. The main source of heat during irradiation is gamma heating. The gas mixture is chosen as to ensure the proper gamma heat extraction at a given temperature, trough a small gap in which the gas is flowing. The main heat transfer modus is conduction. A little part of heat is also extracted by convection, in the flowing gas. To ensure the lowest possible irradiation temperature, all filling materials in the BAGIRA rig are aluminum. This way an irradiation temperature as low as 150°C has been achieved. The temperature was monitored with five thermocouples placed along the rig. The temperature of each

thermocouple was quite stable along the reactor period. The lowest temperature was 140°C and the highest 160°C (Report AEKI, F.Gillemot, G.Uri, 16.04.2004). After the irradiation, only the specimen target is extracted and moved to the hot cells.

- *Experimental Matrix*

The experimental matrix is shown in table 2. Some unirradiated tests are conducted at room temperature, in order have a comparison with the tests conducted at 150°C and also to confirm the good calibration of the measuring system. As explained before, two techniques are used to pre-crack the specimens. One technique uses a high frequency electro-magnetic vibrator. Specimens pre-cracked with this technique are indexed PC. The second technique uses the testing machine itself, and the crack is grown at low frequency. Crack length is controlled using the compliance method. All specimens not marked with PC, have been pre-cracked using the second technique. The specimens irradiated with the high energy protons are all in the *as received* condition. The materials already contain some level of hydrogen, as indicated in table 1. The proton irradiation increases the hydrogen content, as shown in the section 6. The neutron irradiated specimens I14C46 and 69, I25C46 and 49 , I14D40 and I14D45 are all in the *as received* condition. Two specimens loaded with 150 ppm hydrogen have also been irradiated, together with two annealed specimens (8 specimens total, see table 2). The annealed specimens have an hydrogen level close to zero. In this way the synergetic effect of hydrogen and irradiation should be better demonstrated.

Table 2: Experimental Matrix: *The tensile and Charpy specimens were tested at 150°C. Specimens tested at room temperature are indexed RT. The Charpy specimens pre-cracked at high frequency are indexed PC. They have been pre-cracked before the irradiation and experiments. The other specimens were pre-cracked before test at low frequency.*

		Proton Irradiation	Neutron Irradiation
Irradiated	Tensile	1)I31T6, I14T28, I25T12 2)I25T14, I14T27	I14D40, I25D45
	Charpy	3)I25C54 _{PC} , I25C56 _{PC} I25C55 _{PC} 4)I14C54 _{PC} , I14C56 _{PC} I14C53 _{PC}	I14C38-150ppmH2 I25C39-150ppmH2 I14C6-annealed I25C30-annealed I14C46,I14C69,I25C46 I25C49
Unirradiated	Tensile	N31T7 _{RT} , N14T30 _{RT} , N25T16 _{RT} N25T21, N14T32,N31T8 N31T11	N14D50 _{RT} ,N14D51 _{RT} N25D55 _{RT} N14D52,N25D56
	Charpy	N14C99 _{RT} , N14C108b _{RT} N25C98b _{RT} , N25C95b _{RT} N14C105 _{PC} , N25C92 _{PC} , N25C93b, N14C50 _{PC}	N17C33 _{RT} ,N14C102 _{RT} N25C103, N14C57 N25C27 _{PC} -annealed N14C3 _{PC} -annealed N25C36 _{PC} -150ppmH2 N14C34 _{PC} -150ppmH2

5. Specimen Dosimetry

Proton dosimetry

The main radio nuclide produced in titanium by high energy protons is SC46. Unfortunately only unreliable information is available on the production cross sections. HETC predictions (mean of 4 runs in titanium and vanadium) give a cross section of 33.7 mbarns for Ti and 14.4 mbarns for vanadium. Actually about nine different proton and neutron reactions can produce Sc46. With an aluminum sample, the proton fluence can be measured with good accuracy using the well known reaction $^{27}\text{Al} (p,3p3n) ^{22}\text{Na}$. Consequently it was decided to make a dosimetry experiment in which pure aluminum would be irradiated together with both titanium alloys, industrial titanium (#31) and pure titanium. (see Appendice)

Assuming the Al monitor gave the true fluence value and in the case of the experimental set up of the PIREX irradiation head, the evaluated Sc46 cross section is

$$\sigma(\text{Ti}(p,x)) = 27.2 \text{ mbarn}$$

Using the above value, the values for the fluence and displacements per atom have been determined for the irradiated specimens and are listed in table 3.

The dpa cross section for titanium is derived from the classical relation:

$$\sigma_{dpa} = 0.8 \frac{\delta_{E_d}}{2E_T}$$

From HETC calculations in titanium, the damage energy cross section δ_{E_d} has an accepted value of 197.6 barn keV and the displacement threshold energy E_T is given at 30 eV. The above cross-section is then evaluated to 2.63 kbarn. This value corresponds well with data published in the literature for instance in reference [6]. Interesting to note that I25T12, I14T28 and I31T6 were irradiated together and consequently have the same dose. I25T14 and I14T27 were irradiated together with the dosimetry experiment and have a lower dose.

Table 3: *Fluence and displacements per atom after the irradiations in PIREX*

SPECIMEN	Fluence p/cm2	Dose dpa
I25T12	5.09E+19	0.1342
I25T14	1.63E+19	0.0428
I25C55	6.18E+19	0.1628
I25C54	6.16E+19	0.1623
I14T27	2.32E+19	0.0611
I14T28	6.4E+19	0.1685
I14C53	4.96E+19	0.1308
I14C54	4.99E+19	0.1315
I31T6	4E+19	0.1053

Neutron dosimetry

The specimens were irradiated in four reactor cycles for a total of 936 hrs. The first cycle started on June 18, 2002 and the last cycle ended on September 27, 2002. The corresponding saturation factor, considering the natural reaction $^{46}\text{Ti}(n,p)^{46}\text{Sc}$ is 1.558E07 s. The Sc46 activity has been measured in all specimens irradiated in BAGIRA. Assuming a Sc46 production cross section of 13.8mbarn, which was derived from previous analysis in the AEKI reactor, a mean flux of 1.08E20 n/cm2 was calculated, with a standard deviation of only 0.054E20 n/cm2, based on 10 samples.

The dpa cross section in the AEKI reactor, assuming a Watt-Cranberg fission spectrum ($n > 1\text{MeV}$) is 1420 barn.

The estimated dpa is then

$$0.1544 \pm 0.00756 \text{ dpa}$$

The above values seem reasonable. A value of 10.75 mbarn is given for the production cross section of Sc46, in the DOSCROS84 library [Nuclear data guide]. This value is closed to the value proposed for the AEKI reactor. Neutron detectors (Cu, Fe Ni and Nb) have been placed in the BAGIRA rig, very close to our specimens. The analysis of the dosimeters has been done at the AEKI (at the exception of the Nb detector which was not measured) and gave a fast fluence of 4.22E13 n/cm2 s [report Simutis, pos 504 close to our specimens] The resulting fluence (934hrs) would then be 1.42E20 n/cm2. Previous dosimetry analysis in the AEKI reactor gave a fast flux of 2.9E13 n/cm2 s, using the data from the Nb detector [Hegedues, April 2001]. The resulting fluence (934 hrs) would then be 0.975 E20 n/cm2.

To conclude we believe that the dose estimation from the Sc46 activity is correct and gives a fair estimation of the dpa.

6. Hydrogen measurements in the proton irradiated specimens

The hydrogen concentrations after the irradiation in PIREX has been determined in five specimens, using a method based on gas mass spectrometry. The analysis procedure consists of dropping a piece of the specimen under vacuum, into a ceramic crucible heated to 1100°C. Hydrogen release was then measured as a function of time, using a quadrupole mass spectrometer detector [7]. This method allows the measurement of very small specimens having masses between 1 and 2 milligrams. The atomic concentration in *appm* is calculated from the following:

$$C_{appm} = \frac{n_H}{N_{Alloy}} 10^6$$

where N_{Alloy} is the number of atoms per gram in the alloy and n_H the released hydrogen atoms per gram of specimen.

N_{Alloy} is calculated by:

$$N_{Alloy} = \frac{1}{m_u} \sum \frac{X_i}{A_{r,i}}$$

where $A_{r,i}$ is the atomic relative mass of the alloy component i having a weight concentration X_i and m_u is the atomic mass constant.

The conversion to concentration in *wppm* is done according to:

$$C_{wppm} = C_{appm} \times \frac{A_{r,Hydrogen}}{\sum A_{r,i} \times C_i}$$

$$C_{wppm} = C_{appm} \times \frac{\frac{1}{N_H \cdot m_u}}{\frac{1}{N_{Alloy} \cdot m_u}} = C_{appm} \times \frac{N_{Alloy}}{N_{Hydrogen}}$$

C_i is the atomic concentration of each alloy component. The results are shown in table 4. A further experimental analysis based on 4 specimens and 8 measurements, showed that hydrogen intake took place during the original preparation of the specimens. These measurements were conducted separately on unirradiated samples of the same alloy materials that had been cut at EPFL both wet and dry (i.e., with and without water). The results indicated that the wet cutting procedure, using a diamond saw, introduced some hydrogen into the specimens. For alloys 25 and 14, this hydrogen uptake was found to be 14.5 wppm and 7.8 wppm, respectively (average values).

The net hydrogen level, after correction for the hydrogen uptake during cutting, is shown in the last column of table 4. The table suggests two main observations. First the hydrogen is not absorbed at the same rate in both alloys. The Ti6Al4V alloy (Material 25) retains significantly more hydrogen as compared to the Ti5Al2.4Sn

(Material 14). Second, there is no strong specimen size effect, as shown by the comparison of I25T12 which was a 0.34mm flat specimen and the other Charpy specimens (I25C54 and I25C55) which had a cross section of 3x4 mm. Nevertheless I25T12 had the lowest hydrogen level after irradiation among the five samples.

It is also interesting to note that the predicted hydrogen production in titanium is around 650 appm/dpa (Sh. Green, 1984, 126, 30-37), which corresponds to about 14 wppm H/dpa.. The irradiated values of table 4 are for 0.2 dpa. Therefore the observed rates of hydrogen deposition in alloy 14 and 25 were around 70 wppm/dpa and 150 wppm/dpa.- much higher than the prediction. The reason for this significantly higher deposition is currently not known.

Table 4: Measured hydrogen in proton irradiated samples
^aMean and standard deviation (1 σ) of replicate analyses.

Sample	¹ H	Average ^a		Correction	Net ¹ H
	appm	appm	wppm	wppm	wppm
Unirradiated:					
N14C62	3089	2895	62.4	14.5	47.9
	2744	±246	±5.3		
	2574				
	2574				
	3132				
	3194				
	2995				
	2859				
N25C77	1044	1283	28.2	7.8	20.4
	1030	±311	±6.8		
	1164				
	1101				
	1706				
	1652				
Irradiated:					
I14C53	3667	3624	78.1	14.5	63.6
	3581	±61	±1.3		
I14C54	3371	3492	75.2	14.5	60.7
	3613	±171	±3.7		
I25C54	3005	3195	70.2	7.8	62.4
	3385	±269	±5.9		
I25C55	2799	2785	61.2	7.8	53.4
	2771	±20	0.4		
I25T12	2354	2502	55.0	7.8	47.2
	2562	±129	0.6		
	2590				

7.0 Mechanical tests results

7.1 Tensile tests

The results of the tensile tests are given in table 5 for the Ti6Al4V, Ti5Al2.5Sn and titanium Grade 2. As explained in section 4, the neutron experiments use a DIN cylindrical specimen labeled **D** and the proton experiments use a flat specimen labeled **T** in table 4.

All tests have been conducted at the same strain rate, $2.5 \times 10^{-4} \text{ s}^{-1}$. The unirradiated tests have been conducted with both specimen geometries, in order to take into account specimen size effects. The different tensile curves before and after irradiation are given in Fig 2,3 and 4 for the proton irradiation and in Fig 5,6 and for the neutron irradiated specimens.

The specimen geometry has an influence on the tensile properties, as shown in table 5. The stress parameters $R_{p0.2}$ and R_m are slightly higher in the DIN specimens, specially in the Ti5Al2.5Sn alloy. This is clear in the case of N14D52 and N14T32, tested at 150°C.

Table 5: Tensile properties of titanium alloys before and after the proton and neutron irradiation. Strain rate = $2.5 \times 10^{-4} \text{ s}^{-1}$

The specimens labeled ****T**** are flat specimens and were irradiated with protons. The specimens labeled ****D**** are cylindrical solid specimens and were irradiated with neutrons. The first letter in label is a **I** for irradiated or **N** for unirradiated. **DSA** is for Dynamic Strain Ageing and **Stgz** is for Streckgrenze. **Rp0.2** is the 0.2% yield stress, **Rm** the stress at max load, **At** the total elongation, **Z** the reduction of area and **Agt** the uniform elongation.

Titanium Grade 2								
Specimen name	T [°C]	Rp 0.2	Rm	At %	Z %	Agt %	D S A	Stgz
N31T8	150	224.1	305	30.2	19.2	4.8	no	no
N31T11	150	219.8	300.3	28.4	15.5	10.6	no	no
N31T7	21	332.7	482.3	25.6	18.1	10.2	no	no
I31T6	150	355.4	394.5	15.9	N/A	2.1	no	no
Ti5Al2.5Sn								
Specimen name	T [°C]	Rp0.2	Rm	At %	Z %	Agt %	D S A	Stgz
N14T30	20.5	828	951.4	18.9	23.3	11.9	no	no
N14D50	21	831.7	958	17.5	38.8	N/A	v.v.W	N/A
N14D51	21	859.6	975.1	19.5	41.4	13.9	no	no
N14T32	150	636.4	761.5	17.6	21.4	10.2	no	yes
N14D52	150	680.3	814.8	17.3	43.9	9.9	no	yes
I14T28	21	859.6	965.4	14.6	N/A	7.8	no	no
I14T27	150	650.2	753.5	14.6	N/A	6.2	no	no
I14D40	150	800.6	824.4	13.3	N/A	7.5	no	yes
Ti6Al4V								
Specimen name	T [°C]	Rp0.2	Rm	At %	Z %	Agt %	D S A	Stgz
N25T16	20.5	810.3	942.2	17.6	17.9	8.2	no	no
N25D55	21	883.3	946.4	17.8	43.3	10.8	no	no
N25T21	150	629.3	781.5	21.8	19	9.3	no	no
N25D56	150	713.3	795.1	19.6	39.9	10.7	v.v.W	yes
I25T14	150	782.1	800.6	16.5	N/A	3.2	no	no
I25T12	21	990.1	1023.3	9.9	N/A	4.2	no	no
I25D45	150	935.9	946.7	7.6	N/A	2.1	no	yes

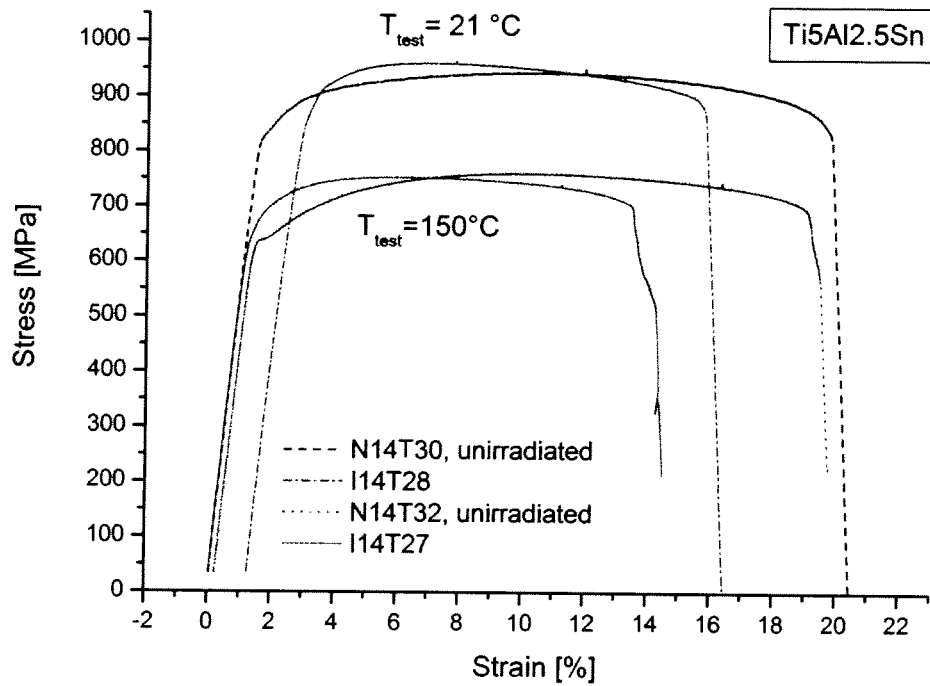


Figure 2. Tensile curves of Ti5Al2.5Sn before and after irradiation with protons at 150°C. I14T28, tested at 21°C has a dose of 0.17 dpa and I14T27 tested at 150°C, has a dose of 0.06 dpa.

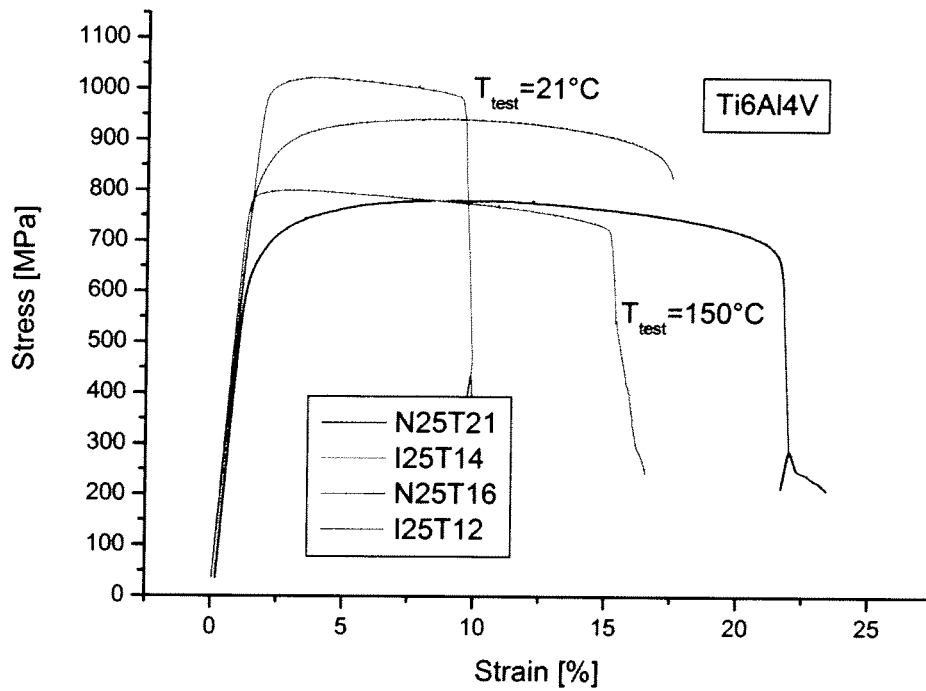


Figure 3. Tensile curves of Ti6Al4V before and after irradiation with protons at 150°C. I25T12, tested at 21°C has a dose of 0.13 dpa and I25T14 tested at 150°C, has a dose of 0.04 dpa.

The total and uniform elongation values are similar in both geometries, whereas the reduction of area is clearly higher in the DIN cylindrical specimens. The Streckgrenze effect (sharp yield point) was visible in both geometries and slightly sharper in the cylindrical geometry.

The comparison of figures 2 and 3 indicates that the alpha alloy is less affected by the irradiation as compared to the alpha +beta alloy. The hardening $\Delta\sigma$ irr at 150°C and 0.06 dpa is only 14Mpa for the alpha alloy as compared to 150 Mpa for the alpha +beta alloy. The hardening $\Delta\sigma$ irr at T test=21°C and 0.13 dpa is clearly larger for the alpha+beta alloy. Furthermore the Ti6Al4V tensile curves have an unstable shape with a low uniform elongation after irradiation. Although less strong in amplitude as compared to what was observed after an irradiation with neutrons at 350°C, the response observed is similar. It is probable that some phase instabilities already occur after the irradiation at 150°C.

Nevertheless at 150°C, the pure titanium is more affected in terms of hardening and ductility loss as can be easily seen from figure 4. The uniform elongation (A_{gt} in table 4) is 2.1% after irradiation. This larger irradiation hardening is a result of the more simple microstructure containing less traps and sinks for the point defects.

Figure 5 presents the effects after the irradiation with neutrons at the same temperature of 150°C, in the alpha alloy. It is interesting to note that the Streckgrenze present in the unirradiated case is reinforced after the irradiation. Nevertheless the material is still able to deform homogeneously and reaches a uniform elongation of 7.5%.

In the Ti6Al4V irradiated with the neutrons, the situation is worst as indicated by the unstable deformation curve of I25D45. The uniform elongation is very low after irradiation, considering that most of the deformation is elastic at the stability limit.

Figures 7 and 8 present the curves before and after irradiation for both alloys at 150°C. The irradiation dose of the proton irradiated specimens is significantly less than the dose reached in the neutron irradiated specimens. Comparing figures 7 and 8, the relative hardening after irradiation appears clearly stronger in the case of the Ti6Al4V alloy, after both the proton and the neutron irradiation. The stronger irradiation hardening in the alpha-beta alloy is probably due to the formation of irradiation induced vanadium precipitates.

In comparing the different curves from protons and neutrons, it seems clear that the protons are less effective in terms of irradiation hardening and reduction of ductility. The hydrogen intake after proton irradiation is of the order of 20 wppm, as shown in table 4. Apparently this increase in the hydrogen level does not modify the tensile properties.

Dynamic strain ageing was not observed during the experiments except in the case of N14D50 and N25D56, where it was qualified as 'very very weak'. Streckgrenze were observed at 150°C only, in both alloys before irradiation and only in the alpha alloy

after irradiation. Nevertheless it is possible that the flow instability shown in the Ti6Al4V was hiding the Streckgrenze.

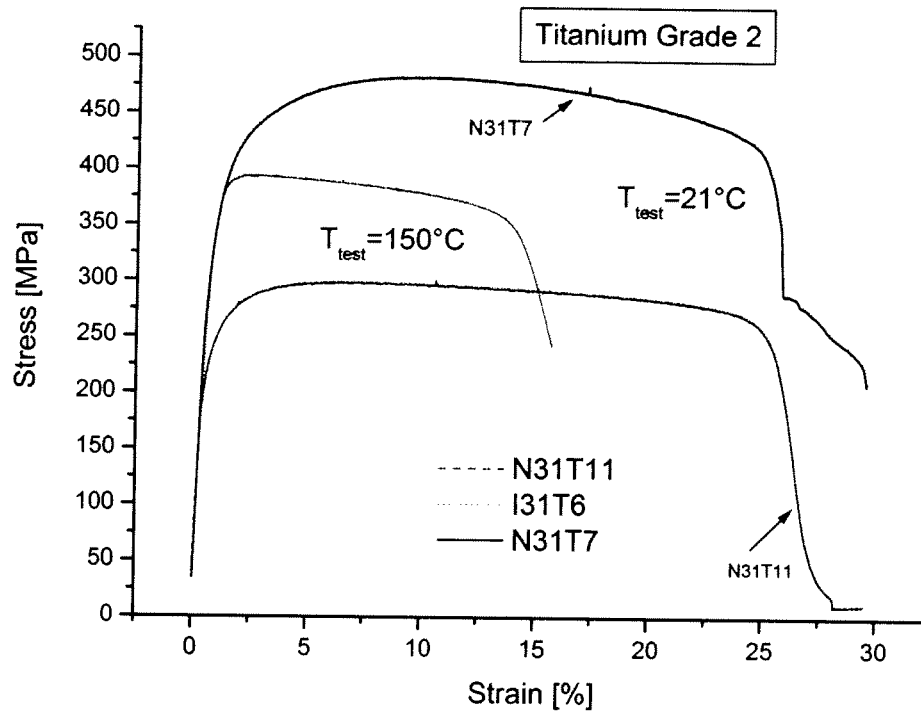


Figure 4. Tensile curves of Grade2 titanium. I31T6 has been irradiated with high energy protons at 150°C , to 0.1 dpa.

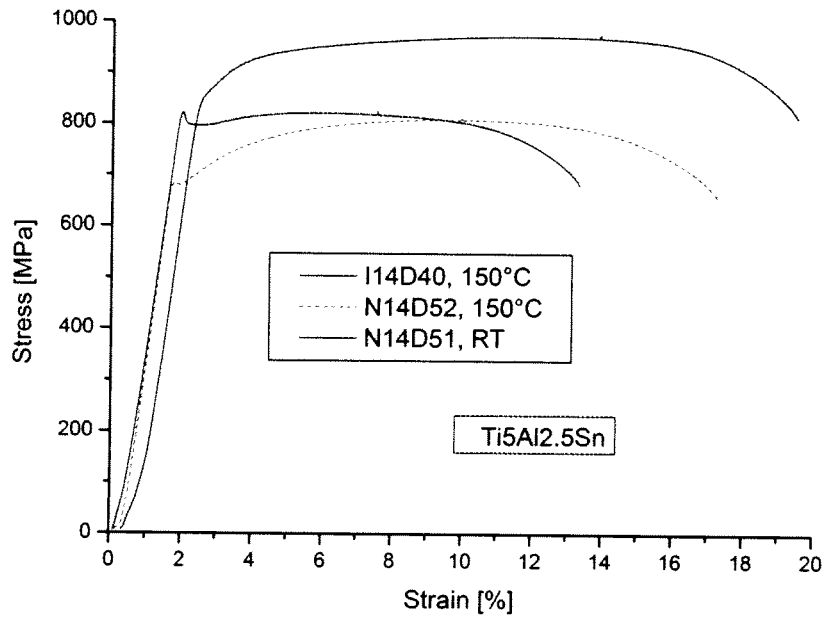


Figure 5. Tensile curves of Ti5Al2.5Sn, irradiated with neutrons at 150°C and 0.15 dpa. The behavior at room temperature is shown for comparison.

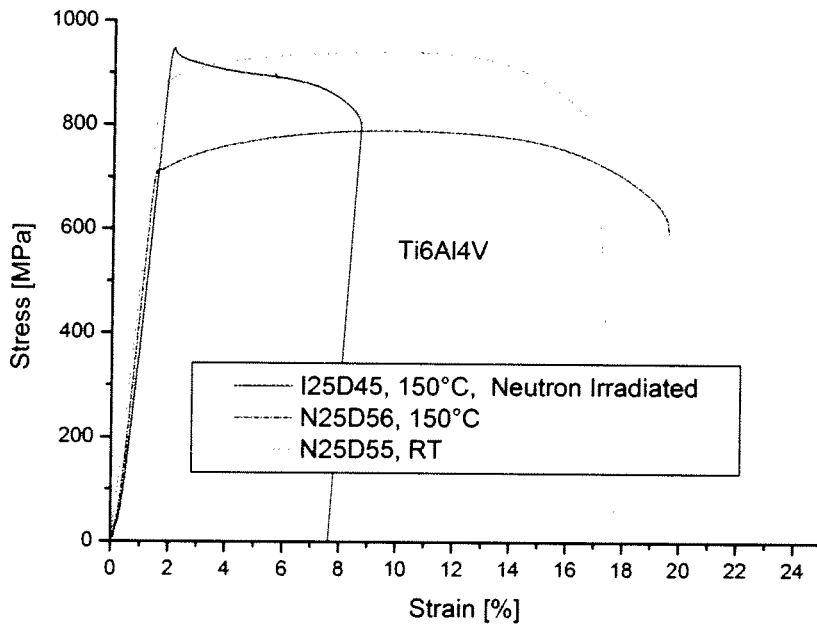


Figure 6. Tensile curves of Ti6Al4V, irradiated with neutrons at 150°C to 0.15 dpa. The behavior at room temperature is shown for comparison.

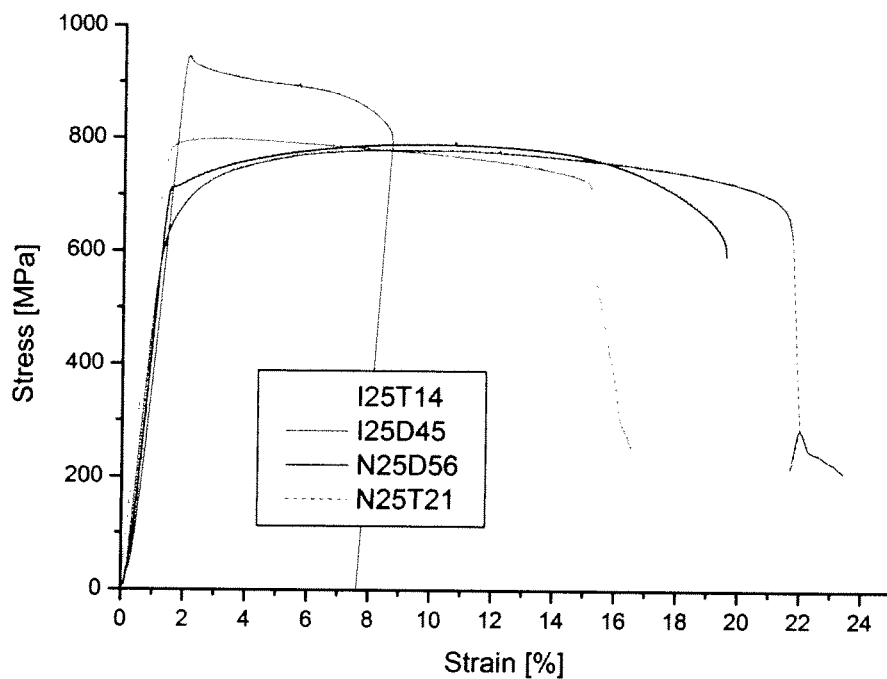


Figure 7. Comparison of tensile curves of Ti6Al4V at 150°C , unirradiated and irradiated with protons (I25T14, 0.043dpa) and neutrons (I25D45, 0.15 dpa) at 150°C

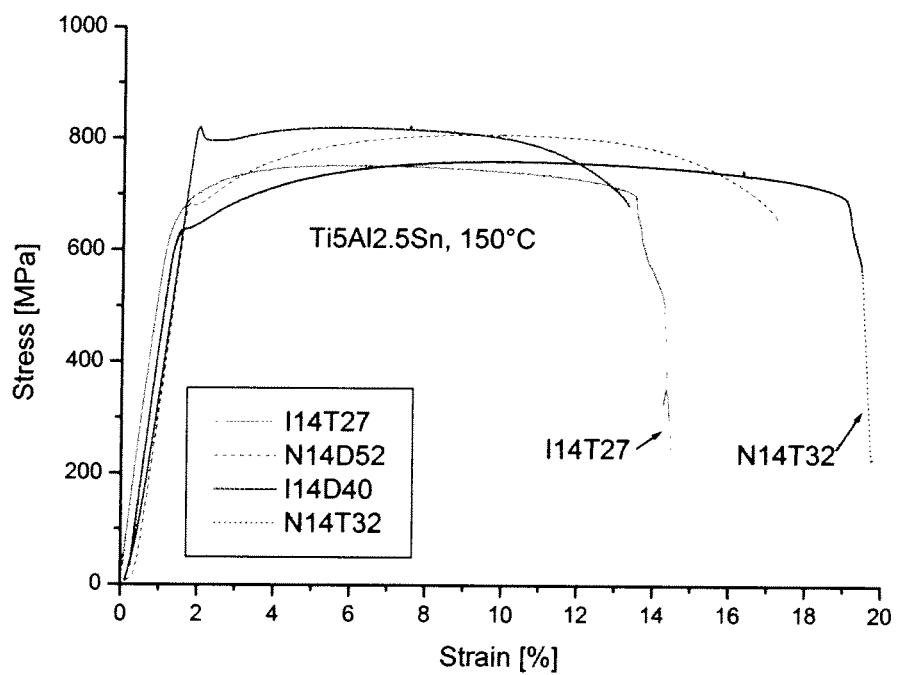


Figure 8. Comparison of tensile curves of Ti5Al2.5Sn at 150°C, unirradiated and irradiated with protons and neutrons at 150°C. I14T27 has 0.06 dpa and I14D40 has 0.15 dpa.

7.2 Fracture toughness tests

The results of the fracture toughness tests is given in table 6. The tests have been accomplished according to the ASTM norm E813. The measurement of crack extension was done using the compliance method which measures the apparent elasticity of the specimen. The effective crack length is then calculated using the compliance transfer relation of Jablonski [8].

All specimens have been loaded with a deformation rate of 8.33×10^{-3} mm/s.

For the unirradiated material, the values of J_Q are very similar in both alloys. The value at RT is around 60 kJ/m^2 for both materials. This is in accordance with previous measurements [9]. The fracture toughness increases at 150°C, to reach a value around 100 kJ/m^2 . The irradiated Ti5Al2.5Sn material is only slightly affected by the irradiation if tested at 150°C, whereas the Ti6Al4V alloy shows a clear reduction in the J_Q value. When tested at RT both irradiated alloys show a large reduction of J_Q . The data are easy to understand if analysed in the light of their hydrogen content. This is shown in figures 9 and 10 where the Ti6Al4V and Ti5Al2.5Sn data are represented as a function of their hydrogen content. As explained previously, hydrogen is already present in the material in the *as received* condition. It was also loaded in a vacuum furnace or removed after annealing in vacuum. The proton irradiation was introducing some hydrogen and the neutron irradiation was not changing the initial content. The results on the hydrogen analysis were presented in section 6 of this report.

For the case of the alpha+beta alloy shown in figure 9, we see that the fracture toughness of the unirradiated material is improved when increasing the temperature from RT to 150°C. It is also improved if the hydrogen content is decreased. Nevertheless the dependence on hydrogen content at 150°C is not strong and for the highest level of the diagram (170 wppm H), J_Q remain of the order of 100 kJ/m^2 . This is more than the value of the *as received* material at room temperature. At RT., the irradiated data show more dispersion than the unirradiated data, an indication for radiation embrittlement. The proton irradiated data fit quite well the trend of the neutron irradiated data. Since the fracture toughness of the 150wppm H loaded material is clearly lower after than before irradiation, we can argue that the damage from the irradiation and from the hydrogen are additive.

The data for the alpha alloy are presented in figure 10. They show a similar behavior. At 150°C, as the hydrogen content increases, the fracture toughness decreases, whereas in the unirradiated material a reverse response is observed. This behavior is in fact not a consequence of the hydrogen impurity atoms but rather a consequence of

the microstructural changes introduced by the hydrogen charging (see report [9]). Despite the toughness improvement observed at 150°C and 150wppmH, after neutron irradiation a drastic decrease of toughness is observed. Nevertheless the value is approximately four times higher, as compared with the Ti6Al4V case. The proton irradiated data are slightly lower than the neutron irradiated data, when plotted against their hydrogen content (see figure 10).

The lowest fracture toughness value is measured at RT, after proton irradiation.

Comparing Fig. 9 and 10, it seems that the Ti6Al4V data show more dependence on hydrogen level, as compared to the Ti5Al2.5Sn data. It is possible that more hydrides are present in the alpha+beta alloy, due to a different solubility limit. At higher temperatures, the hydrides are expected to be dissolved [10].

The fractographs of the unirradiated and irradiated specimens have been analyzed under the scanning electron microscope. The general aspect of all fractographs is ductile. Relatively large effects are measured in the mechanical test but the difference does not show up in the appearance of the fractographs. This is shown in Figures 11 and 12 which compare two extreme cases, I25C54 irradiated at 150°C and showing a low J_Q value and N25C95b unirradiated and having a relatively high J_Q value. Both fractographs show a fracture surface with dimples indicating large local deformations.

Table 6: Crack initiation fracture toughness values J_Q in kJ/m² before and after irradiation in PIREX and BAGIRA. In the first column, the specimens irradiated in BAGIRA are labeled n and the specimens irradiated in PIREX are labeled p. Some specimens were pre-cracked before testing and irradiation. This is indicated with PC in the 7th column. The last column indicate if crack growth was observed during testing.

Spec. Name	Condition	T _{irr} [°C]	Dose [dpa]	T _{test} [°C]	J _Q	Pre-cracked	Crack Propagation
Ti6Al4V							
N25C95b	as received	N/A	N/A	22	64.1		yes
N25C98b	as received	N/A	N/A	22	59.6	PC	yes
N25C93b	as received	N/A	N/A	150	125		no
N25C92b	as received	N/A	N/A	150	108.9	PC	yes
N25C103	as received	N/A	N/A	150	113		no
N25C36	150wppmH	N/A	N/A	150	82.6	PC	yes
N25C27	annealed	N/A	N/A	150	220	PC	no
I25C30,n	annealed	150	0.154	150	68.2		yes
I25C39,n	150wppm H	150	0.154	150	22.1		yes
I25C54,p	as received	150	0.162	22	15.7	PC	yes
I25C55,p	as received	150	0.163	150	36.6	PC	yes
I25C56,p	as received	150	0.162	150	31.7	PC	yes
I25C49,n	as received	150	0.154	150	44.7		yes
I25C46,n	as received	150	0.154	150	14.3		yes
Ti5Al2.5Sn							
N14C108b	as received	N/A	N/A	22	65.1		yes
N14C102	as received	N/A	N/A	22	60.3		yes
N14C99b	as received	N/A	N/A	22	44.5		yes
N14C105b	as received	N/A	N/A	150	67.2	PC	yes
N14C50b	as received	N/A	N/A	150	108.4	PC	yes
N14C3	annealed	N/A	N/A	150	152		no
N14C57	as received	N/A	N/A	150	81.6	PC	yes
N14C34	150wppm H	N/A	N/A	150	180	PC	no
I14C38,n	150wppm H	150	0.154	150	82.8		yes
I14C6,n	annealed	150	0.154	150	110		no
I14C56,p	as received	150	0.131	150	59.6	PC	yes
I14C54,p	as received	150	0.131	150	66.2	PC	yes
I14C53,p	as received	150	0.131	22	16.8	PC	yes
I14C69,n	as received	150	0.154	150	67		yes
I14C46,n	as received	150	0.154	150	93.4		yes

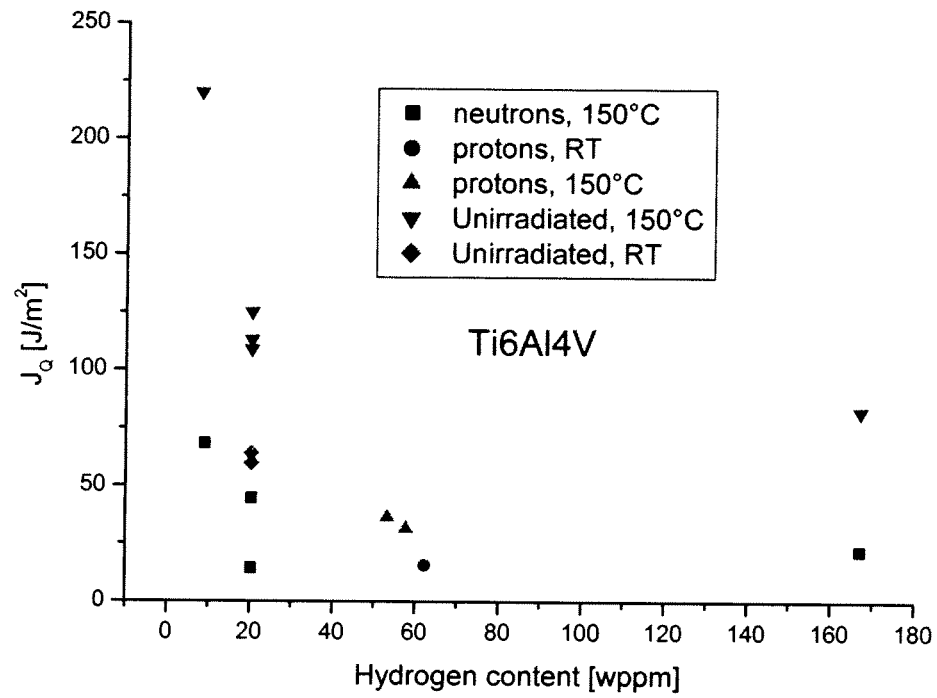


Figure 9. Fracture toughness of Ti6Al4V alloy, unirradiated, irradiated at 150°C, with protons to 0.163 dpa and neutrons to 0.154 dpa. The data are plotted as a function of their hydrogen level.

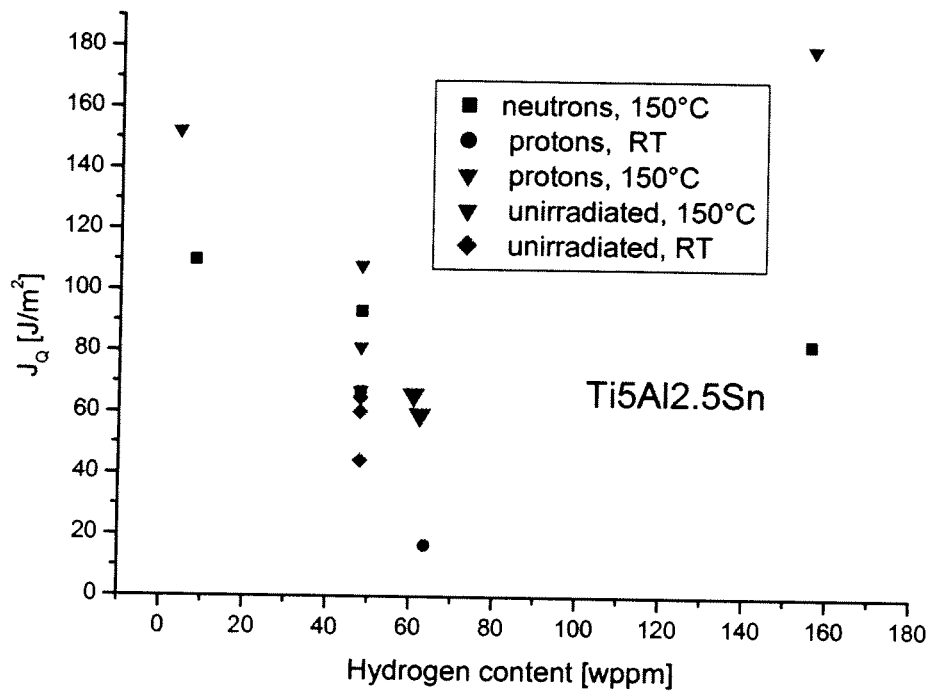


Figure 10. Fracture toughness of Ti5Al2.5Sn alloy, unirradiated, irradiated at 150°C, with protons to 0.131 dpa and neutrons to 0.154 dpa. The data are plotted as a function of their hydrogen level.

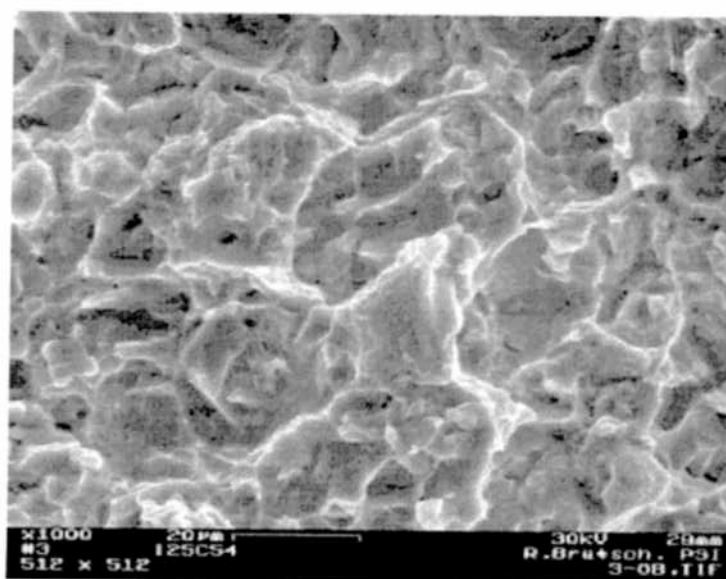


Figure 11. Fractograph of the irradiated specimen I25C54 with J_Q value of 16 kJ/m^2

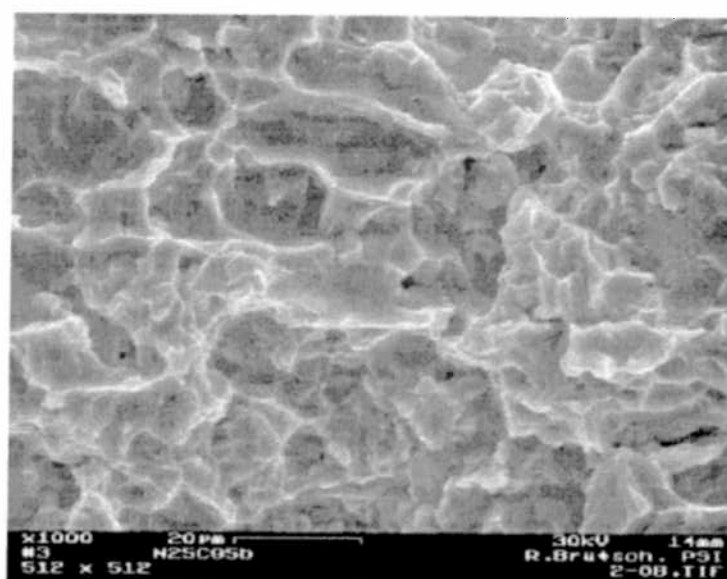


Figure 12. Fractograph of the unirradiated specimen N25C95b with J_Q value of 64 kJ/m^2

8. Conclusions

Tensile and fracture toughness specimens of Ti6Al4V , Ti5Al2.5Sn and Titanium Grade 2 have been irradiated with high energy protons to a dose between 0.04 and 0.17 dpa, at 150°C. Tensile and fracture toughness specimens of Ti6Al4V , Ti5Al2.5Sn, some of them loaded with hydrogen, have been irradiated with neutrons at 150°C, to 0.15dpa.

The tensile tests seem to indicate that the Ti6Al4V is more affected by the irradiation as compared with the Ti5Al2.5Sn alloy. There is more hardening and ductility reduction in the Ti6Al4V alloy. The irradiation seems to induce the precipitation of vanadium rich precipitates. Nevertheless the general behaviour of the alpha beta alloy remains ductile.

The irradiation hardening and the reduction in ductility are more pronounced at 150°C in the pure titanium.

Compared on a dpa base, the neutrons seem more damage effective than the protons, in terms of ductility loss.

The crack initiation fracture toughness values are strongly reduced after irradiation, especially when tested at room temperature. At 150°C the reduction in toughness is more pronounced in the Ti6Al4V alloy. Nevertheless the fractographs indicate a ductile fracture for all conditions in both materials.

The fracture toughness data can be well understood, if represented as a function of their hydrogen content. Hydrogen levels up to 150wppm have moderate effect on toughness, at a test temperature of 150°C. For the irradiated specimens in both alloys, increasing the hydrogen content decreases the fracture toughness.

The neutron and proton fracture toughness data show a consistent behaviour, when compared in relation to their associated hydrogen content.

Acknowledgements:

The Paul Scherrer Institute at Villigen, PSI, is sincerely thanked for its logistical and technical support throughout this project..

REFERENCES:

1. Marmy, P., et al., *Tensile and Fatigue Properties of two Titanium Alloys as Candidate Materials for Fusion Reactors*. Journal of Nuclear Materials, 2000. 283-287: p. 602-606.
2. Marmy, P. and T. Leguey, *Impact of irradiation on the tensile and fatigue properties of two titanium alloys*. Journal of Nuclear Materials, 2001. 296: p. 155-164.
3. Marmy, P., et al., *The tensile and fatigue behaviour of the titanium alloys Ti6Al4V and Ti5Al2.5Sn before and after irradiation with protons to doses up to 0.3 dpa*. 2001, CRPP-EPFL: Lausanne. p. 1-46.
4. Tähtinen, S., et al., *Tensile and fracture toughness properties of unirradiated and neutron irradiated titanium alloys*. Journal of Nuclear Materials, 2002.
5. Leguey, T., et al., *Microstructure of Ti5Al2.5Sn and Ti6Al4V deformed in tensile and fatigue tests*. Journal of Nuclear Materials, 2002. 305: p. 52-59.
6. Barnett, M.H., et al. in *3rd International Topical Meeting on Nuclear Applications of Accelerator Technology (AccApp99)*. 1999.
7. Oliver, B.M., et al., *Quadrupole Mass Spectrometer System for the Determination of Low Levels of Hydrogen in Irradiated Materials*. Journal of Nuclear Materials, 2001. 283-287: p. 1006.
8. Jablonski, D.A., et al., *Compliance Functions for Various Fracture Mechanics Specimens*. Engineering Fracture Mechanics, 1985. Vol. 22(No 5): p. 819-827.
9. Marmy, P., et al., *The effect of hydrogen on the fracture toughness of the titanium alloys Ti6Al4V and Ti5Al2.5Sn before and after neutron irradiation*. 2003, CRPP, Centre de Recherches en Physique des Plasmas, EPFL Lausanne. p. 1-27.
10. O.Kubaschewski, et al., *Titanium: Physico-Chemical Properties of its Compounds and Alloys*, ed. A.E. Review. Vol. Special Issue No.9. 1983: International Atomic Energy Agency, Wagramerstrasse 5, P.O. Box 100, A-1400 Vienna, Austria. 460.

JUNE 2004 (Revised version)

PROTON INTEGRATED CURRENT AND DPA DETERMINATION FOR TITANIUM SAMPLES IRRADIATED AT PIREX

Dr. F. Hegedüs

1. Titanium samples irradiated at PIREX

Beam on: 17.05.02 19h20

Beam out: 19.05.02 16h17

Proton dose : 1.544 As

Sample surface: $20 \times 4.9 \text{ mm}^2 = 0.98 \text{ cm}^2$

1.1. List of irradiated samples

sample	thickness (approx)mm	Ti %	Al %	sample mass mg	number of Ti atoms in sample	number of Al atoms in sample
Ti30 pure	0.115	100	---	55.7	7.143E+20	-----
Al00 pure	0.161	----	100	37.0	-----	8.250E+20
Ti25 alloy	0.177	90.0	6.08	74.1	8.381E+20	1.005E+20
Ti14 alloy	0.176	92.6	5.0	75.7	8.810E+20	8.610E+19
Ti31 ind.	0.270	100	---	120.0	1.539E+21	-----

1.2. Counting of 46Sc(83.80d) and 22Na(950.4d) activities

	46Sc activity [Bq] counted: 01.10.02, 12h	22Na activity [Bq] counted: 01.10.02, 12h	46Sc activity[Bq]EOB per nat.Ti atom in the irradiated mass	22Na activity[Bq]EOB per nat.Al atom in the irradiated mass
Ti30	5.831E+06	4.47E+04	1.236E-13	-----
Al00	-----	5.37E+05	-----	3.588E-15
Ti25	3.582E+06	7.98E+04	6.473E-14	4.367E-15
Ti14	3.444E+06	6.60E+04	5.919E-14	4.416E-15
Ti31	3.043E+06	2.17E+04	2.995E-14	-----

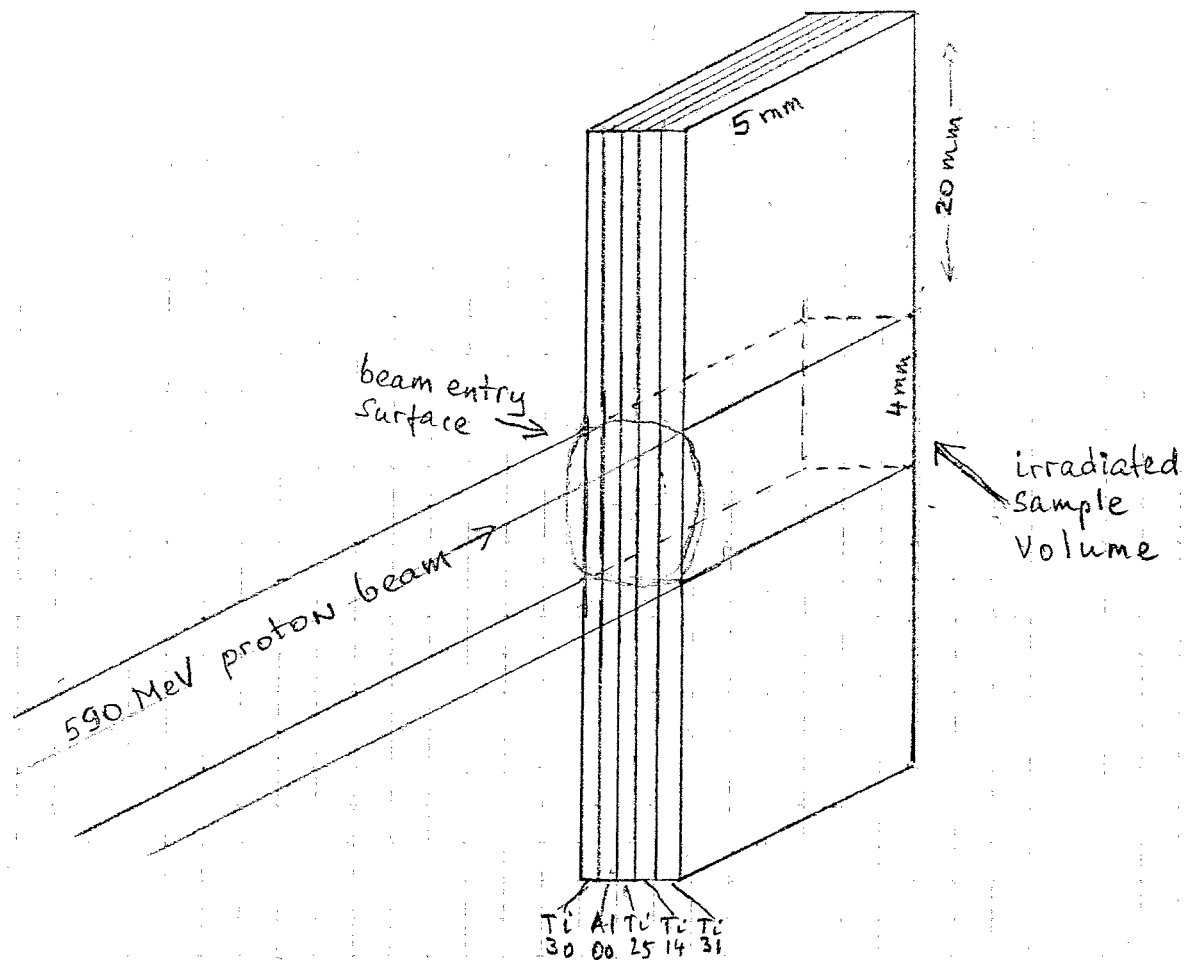
Elapsed time between EOB and counting :134 d

Decay correction for 46Sc : 3.029, for 22Na :1.103

1.3. Irradiation conditions

It is assumed that the beam had an ellipsoidal section, vertical height:4 mm, horizontal width:3 mm and entered frontally into the target sandwich (see layout below). Therefore the irradiated mass was 1/5 part of the total sample mass.

1.4. Layout of the samples during irradiation



2. Integrated proton current determination by means of the $^{27}\text{Al}(p, 3p3n)^{22}\text{Na}$ monitor reaction

To measure the proton current in the energy range of $500 < E < 600$ MeV, the $^{27}\text{Al}(p, 3p3n)^{22}\text{Na}$ monitor reaction is the best adapted (Ref.1.). The activation cross section: $\sigma(590 \text{ MeV}) = 14.0 \pm 0.3 \text{ mbarn}$ is well known since 1963 (Ref.2.). During the last 30 years it was many times remeasured and confirmed (Ref.3.). In the position Al00 (second from left, at 0.20 mm) the integrated proton current was calculated.

Integrated proton current, I_t (dimensionless), is the number of protons traversed the irradiated sample volume, can be calculated by :

$$I_t[-] = A[s^{-1}] * S[\text{cm}^2] / \{N[-] * \sigma[\text{cm}^2] * \lambda[s^{-1}]\}$$

Where:

A : monitor activity at EOB [s^{-1}]

S : irradiated sample surface, perpendicular to the beam direction [cm^2]

σ : monitor reaction cross section [cm^2]

N : number of atoms involved in the monitor reaction in the irradiated volume
dimensionless [-]

λ : decay constant [s^{-1}]

Substituting into the formula :

$$A = 5.92\text{E}+05, S = 0.00644, N = 1.65\text{E}+20, \sigma = 14.0\text{E}-27, \lambda = 8.441\text{E}-09$$

$$I_t = 1.955\text{E}+17$$

3. Determination of the integrated proton current by means of the reaction $^{nat}\text{Ti}(p,x)^{46}\text{Sc}$

The following proton reactions can produce ^{46}Sc :

(nat.abou.:7.5%) $^{47}\text{Ti}(p,2p)$
 (nat.abou.:73.7%) $^{48}\text{Ti}(p,2pn)$ or $(p,^3\text{He})$
 (nat.abou.:5.4%) $^{49}\text{Ti}(p,2p2n)$ or $(p,^4\text{He})$
 (nat.abou.:5.2%) $^{50}\text{Ti}(p,2p3n)$

Additionally if neutrons are present, they can also produce ^{46}Sc :

(nat.abou.:8.3%) $^{46}\text{Ti}(n,p)$
 (nat.abou.:7.5%) $^{47}\text{Ti}(n,pn)$ or (n,d)
 (nat.abou.:73.7%) $^{48}\text{Ti}(n,p2n)$ or (n,t)
 (nat.abou.:5.4%) $^{49}\text{Ti}(n,p3n)$
 (nat.abou.:5.2%) $^{50}\text{Ti}(n,p4n)$

Consequently the total cross section, $^{nat}\text{Ti}(p \text{ or } n, x)$ depends on the strength of the secondary particle field (lower energy spallation protons and neutrons). The contribution of a reaction to the total cross section depends on the natural abundance of the target isotope, on the magnitude of the cross section and on the energy of the bombarding particle. E.g. in the case of 590 MeV protons only two reactions, $^{48}\text{Ti}(p,^3\text{He})$ and $^{49}\text{Ti}(p,^4\text{He})$ are important. The reason is they are emitting by spallation complete nuclids as ^3He and ^4He . Considering the high isotopic abundance of ^{48}Ti , in this process the predominant reaction is $^{48}\text{Ti}(p,^3\text{He})$.

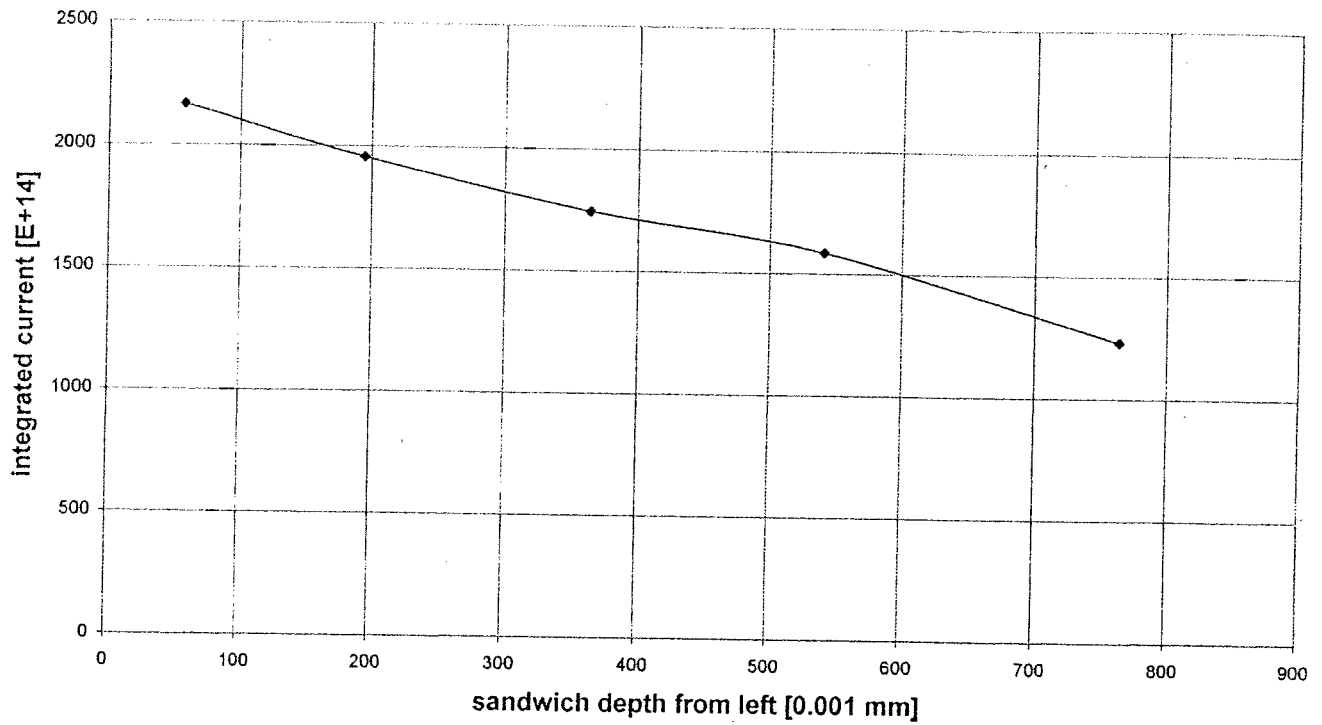
Unfortunately there are not useful published data of these reaction cross sections. The only available cross section for 590 MeV protons is given in the Report Hegedüs, (June 6, 1990) $\sigma(^{nat}\text{Ti}(p,x)) = 29.3 \text{ mbarn}$. Substituting this σ value into the I_t formula (see above), the following integrated current values have been obtained (see 5-th column in table below):

position	sample sandwich mid-depth from left [mm]	S[cm ⁻²] Irra-diated area	N [-] Number of atoms in irradiated volume	Integr. proton current with $\sigma = 29.3 \text{ mb}$	Integr. proton current with $\sigma = 27.2 \text{ mb}$
Ti30	0.057	.00460	1.429E+20	2.015E+17	2.164E+17
Al00	0.195	.00644	1.650E+20	1.955E+17*	1.955E+17*
Ti25	0.364	.00708	1.676E+20	1.624E+17	1.744E+17
Ti14	0.541	.00704	1.762E+20	1.477E+17	1.586E+17
Ti31	0.764	.01080	3.078E+20	1.146E+17	1.231E+17

(*) measured with Al monitor, normalization

Assuming that the integrated current obtained by means of the $^{27}\text{Al}(p,3p3n)^{22}\text{Na}$ monitor reaction is more reliable than the these by Ti reactions, the integrated proton current values have been normalized to the Al value (1.955E+17 in position Al00). The arithmetic mean value of positions Ti30 (2.015E+17) and Ti25 (1.624E+17) 1.820E+17 is slightly less than the measured Al value. The ratio of the two values is 1.075. Therefore it seems the used 29.3 mbarn is too high, 27.2 mbarn gives compatible results (see 6-th column in table before and the diagram on the next page).

Integrated proton current vs. sandwich depth from left



4.dpa calculation

4.1.Review of dpa cross sections for 590 MeV protons

source	σ_{dpa} in Fe	σ_{dpa} in Ti
SPECTER code calculated by L.Greenwood	17 kbarn	23.4 kbarn
VNMTTC code from Los Alamos	3.8 kbarn	---
HETC code calculated by Sh.Green	---	2.63 kbarn
HETC code (Ref.4&5)	2.65 kbarn	---

4.2.Calculation of dpa

Using the damage cross section calculated with HETC code where

$\sigma_{\text{dpa}}(590 \text{ MeV})=2.65 \text{ kbarn}$, dpa for each sample position was calculated by means of the following formula :

$$\text{dpa}[-] = \text{It}[-] * \sigma_{\text{dpa}}[\text{cm}^2] / S[\text{cm}^2]$$

position	dpa
Ti30	0.1247
Ti25	0.0652
Ti14	0.0597
Ti31	0.0302

References

1. F.Hegedüs int.report June 6.1990.
2. Heydegger et al. Phys.Rev.C14,1506 (1976)
3. R.Michel et al. Nucl.Inst.Met.Phys.Res. B129(1997)
4. M.James, Ph.Ferguson in press
5. M.H.Barnett et.al.in Proceedings of the 3rd International Topical Meeting on Nuclear Applications of Accelerator Technology (AccApp99) p.555